

Importance of the additional step-edge barrier in determining film morphology during epitaxial growth

J. A. Meyer

Abteilung Oberflächenchemie und Katalyse, Universität Ulm, D-89069 Ulm, Germany

J. Vrijmoeth

*Abteilung Oberflächenchemie und Katalyse, Universität Ulm, D-89069 Ulm, Germany
and Department of Applied Physics and Materials Science Centre, University of Groningen, Nijenborgh 4,
9747 AG Groningen, The Netherlands*

H. A. van der Vegt and E. Vlieg

*Stichting voor Fundamenteel Onderzoek der Materie, Institute for Atomic and Molecular Physics, Kruislaan 407,
1098 SJ Amsterdam, The Netherlands*

R. J. Behm

Abteilung Oberflächenchemie und Katalyse, Universität Ulm, D-89069 Ulm, Germany

(Received 4 April 1995)

A model of epitaxial growth based on steady-state assumptions is derived and shows that the decisive quantity determining the film morphology is the *additional* energy barrier at the step edges, i.e., the barrier to descend the step minus the surface-diffusion barrier. The model allows this barrier to be directly determined from experimentally observed film morphologies. It is applied to homoepitaxy on Ag(111) and Pt(111) where the additional barriers amount to ~ 150 and ~ 165 meV, respectively. In addition, this model provides new understanding of more complex processes, such as the surfactant effect of Sb on Ag(111) and reentrant growth on Pt(111).

There has been continued interest in epitaxial growth with the parallel goals of obtaining both a more fundamental understanding of the growth and improving control to obtain new materials with desirable properties.¹ While homoepitaxial growth has limited prospects for the latter, its simple thermodynamics makes it useful for the former. In spite of the apparent triviality of homoepitaxial systems, recent experiments have shown a surprising variety of behaviors, including reentrant layer-by-layer growth² and the change in growth morphology with surface active species.³⁻⁶ Although it was immediately recognized that the energy barrier for adatoms to move over step edges and the shape of the island perimeter play an important role in determining the film morphology,^{2,4,7} an analytic model capable of explicitly showing the relative importance of these factors has not been presented. Here we develop such a model which allows the energy barrier for adatoms to move over descending step edges to be calculated directly from STM (scanning tunneling microscopy) or LEEM (low-energy electron microscopy) observations. An accessible experimental determination of this decisive barrier is of obvious importance for learning to control epitaxial growth and for comparing results from simulations and first-principle calculations. We demonstrate the use of this model by analyzing homoepitaxy on Ag(111) and Pt(111) and obtain step edge barriers of 150 and 165 meV in excess of the terrace diffusion barriers, respectively. Additionally, this model is used to analyze the associated problems of the role of Sb additives on Ag(111) homoepitaxy⁸ and reentrant growth in Pt(111) homoepitaxy.^{2,7}

The onset of vertical growth, i.e., the nucleation of the second layer, can occur in three different stages of the first-layer growth process: (i) in the transient regime where the first-layer island density builds up, (ii) in the region of saturated island density, or (iii) in the coverage domain above the onset of coalescence, where the density of first-layer islands decreases. The actual situation is largely determined by the amount of interlayer transport and hence by the relative size of the barrier for diffusing over island edges. In the absence of an additional repulsive barrier at island edges, second-layer islands will not occur until the onset of first-layer island coalescence and layer-by-layer growth results. In contrast, the observation of second-layer nucleation for Ag/Ag(111) (Ref. 8) and Pt/Pt(111) (Ref. 7) before the onset of coalescence indicates a significant additional barrier at steps for these systems.

For modeling the growth with an additional edge barrier we assume that at time t deposition has led to the build-up of three-dimensional (3D) islands consisting of a number of concentric circles with decreasing radius R_n . Following the notation of Cohen *et al.*,⁹ the occupancy of the n th layer θ_n as a function of time at deposition rate $1/\tau$ obeys the set of differential equations

$$\frac{d\theta_n}{dt} = \frac{1 - \alpha_{n-1}}{\tau} (\theta_{n-1} - \theta_n) + \frac{\alpha_n}{\tau} (\theta_n - \theta_{n+1}). \quad (1)$$

α_n represents the amount of interlayer transport; it denotes the fraction of atoms which diffuse over the step and attach to this level after landing on top of level n . Its value,

in the work by Cohen *et al.*,⁹ was defined as $\alpha_n = A[d_n / (d_n + d_{n+1})]$; A is an adjustable parameter between 0 and 1 and d_n the perimeter of the n th-layer island. We derive this expression explicitly here as follows. First, all adatoms landing on the *topmost* layer move over the island edge and attach to it. This continues as long as the coverage θ_n of that layer is smaller than some critical value θ_c . That is, α_n is set to 1 for $\theta_n < \theta_c$. A next-higher-layer island is created as soon as θ_c is reached.⁶ θ_c is directly available from STM or LEEM images. Second, after a next-higher-layer island has nucleated, α_n is calculated using steady-state assumptions. As in the work of Stoyanov and Markov,¹⁰ the adatom density $\rho(r)$ at a distance r from the center of a layer is given by equations which relate the number of atoms impinging on the surface between R_{n+1} and r to the sum of the number of atoms diffusing outward past r and of those being attached to level $n+1$:

$$\frac{1}{\tau} \pi(r^2 - R_{n+1}^2) = 2\pi R_{n+1} \rho(R_{n+1}) h - 2\pi r h \frac{d\rho(r)}{dr}. \quad (2)$$

A similar equation applies for the region between r and R_n ,

$$\frac{1}{\tau} \pi(R_n^2 - r^2) = 2\pi r h \frac{d\rho(r)}{dr} + 2\pi R_n \rho(R_n) s. \quad (3)$$

All radii are given in lattice constants. The terms $h = \exp(-E_d/kT)$ and $s = \exp(-E_s/kT)$ denote the probabilities for hopping on flat terraces and over descending step edges, respectively. Using conservation of number of atoms landing on level n ,

$$\frac{1}{r} \pi(R_n^2 - R_{n+1}^2) = 2\pi R_{n+1} \rho(R_{n+1}) h + 2\pi R_n \rho(R_n) s,$$

allows $\rho(R_n)$ and $\rho(R_{n+1})$ to be calculated. The fraction of atoms which attach to level n is proportional to $s\rho(R_n)R_n$ and the fraction attaching to level $(n+1)$ is proportional to $h\rho(R_{n+1})R_{n+1}$. With these boundary conditions, integration of (2) and (3) yields α_n :

$$\alpha_n = \frac{R_n^2 - r^{*2}}{R_n^2 - R_{n+1}^2}, \quad (4a)$$

where r_n^* is defined as the intermediate radius where the adatom density is maximum,

$$r_n^{*2} = R_{n+1}^2 + R_n^2 \times \left\langle \frac{(R_n^2 - R_{n+1}^2) \left(\frac{h}{R_n s} + \frac{1}{2} \right) - R_{n+1}^2 \ln \left[\frac{R_n}{R_{n+1}} \right]}{1 + R_{n+1} \ln \left[\frac{R_n}{R_{n+1}} \right] + \frac{R_{n+1}}{R_n} \left(\frac{h}{s} \right)} \right\rangle. \quad (4b)$$

Note that when the barrier to move over a step edge becomes very large, $r_n^* \Rightarrow R_n$ which gives $\alpha_n = 0$ and the layer distribution expected for Poisson growth. In α_n , the hopping rates h and s appear only in a ratio. *This demonstrates that it is the difference between the hopping barriers on the terrace*

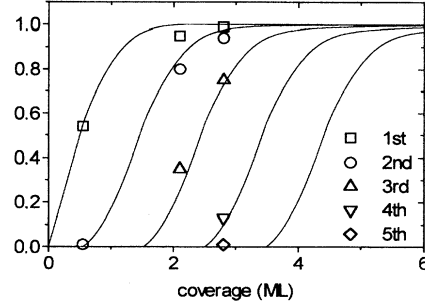


FIG. 1. Layer completion as a function of coverage calculated for an additional barrier of $\Delta s = 150$ meV. The layer occupancies indicated by the symbols are taken directly from STM images.

and the step edges (the “additional barrier” defined as $\Delta s = E_s - E_d$) which determines the amount of interlayer transport and thus the smoothness of the growing film. As shown below for Ag(111) and Pt(111) this model allows the direct determination of this barrier from STM images. Perhaps more importantly, however, is the philosophical implication of this result in that it shows that an increase in diffusion barrier simultaneously on all growing layers leads to more transport between layers and hence a smoother film. This perhaps somewhat counterintuitive result has not been formulated previously, to the best of our knowledge, and contrasts the description recently put forth by Zhang and Lagally, which predicts that growth will become rougher with increasing diffusion barrier on the terraces and a constant total barrier at steps.¹¹

The layer coverage as a function of deposited material is obtained by numerically solving Eq. (1), using α_n from (4), and can be fitted to the experimentally observed values. In Fig. 1, this is demonstrated for the case of the homoepitaxy of Ag/Ag(111). With $\theta_c = 0.55$ ML, as obtained from STM images,^{8,12} the best fit to the layer occupancies as observed using STM is obtained with an additional barrier $\Delta s = 150 \pm 20$ meV.¹³

We now modify the model to consider the onset of second-layer nucleation. This simplified analysis provides a readily applicable estimate of the additional barrier at step edges and allows the effect of different diffusion barriers on different layers to be assessed. The latter may be expected to be important for systems with surfactants and also for heteroepitaxial systems.¹⁴ A second-layer island nucleates when a first-layer island reaches a critical size $R_{1,c}$.⁶ This is equivalent to the condition that the 2D adatom density reaches a critical value ρ_c . The density on top of a first-layer island before second-layer nucleation occurs is found by using Eq. (2) with $R_{n+1} = 0$ and replacing h with h_1 , the hopping probability on a first-layer island:

$$\pi r^2 = -2\pi r \tau h_1 \frac{d\rho}{dr}. \quad (5)$$

Integration shows that the adatom density on top of the island has a parabolic radial dependence. Employing conservation of number of atoms yields for the density at the center of the first-layer island:

$$\rho(0) = \frac{R_1^2}{4\tau h_1} + \frac{R_1}{2\tau s}. \quad (6)$$

The critical 2D gas density ρ_c can be estimated from the first-layer island density. Immediately after the saturated first-layer island density is reached, the 2D gas density between first-layer islands will be just below ρ_c . Thus, an approximation is obtained by starting with Eq. (6) and replacing (i) both s and h_1 with h_0 (the hopping probability on the substrate) and (ii) $R_{1,c}$ with $R_{0,c}$, a measure of the spacing between the centers of first-layer islands:

$$\rho_c \cong \frac{R_{0,c}^2}{4\tau h_0} + \frac{R_{0,c}}{2\tau h_0}. \quad (7)$$

$R_{0,c}$ is difficult to determine analytically with precision due to the lack of symmetry of the first-layer islands. We estimate that it is between $D/2$ and D , with D the average distance between first-layer islands. Equating (6) and (7) with $\rho(0) = \rho_c$ for $R_1 = R_{1,c}$ and rearranging yields

$$\left(\frac{R_{0,c}}{R_{1,c}}\right) = \left(\frac{h_0}{h_1} + \frac{2h_0}{R_{1,c}s}\right)^{1/2} = \left(\frac{h_0}{h_1} + \frac{2\exp(\Delta s/kT)}{R_{1,c}}\right)^{1/2}. \quad (8)$$

This equation yields an estimate of the additional barrier at the edges (Δs) from the radii, $R_{0,c}$ and $R_{1,c}$, observed at the onset of second-layer nucleation. Their ratio $R_{0,c}/R_{1,c}$ is close to 1.0 for smooth growth and larger than roughly 1.5 for cluster growth. This has a meaning similar to the “ F factor” in the model of Zhang and Lagally.¹¹

We apply Eq. (8) to determine the additional barrier Δs for the cases of Ag(111) and Pt(111). The error in these results is dominated by that in the approximation $D/2 < R_{0,c} < D$. For Ag(111), we obtain values for $R_{0,c} = D/2 = 200$ nm and $R_{1,c} = 100$ nm from STM images^{8,12} or $R_{0,c}/R_{1,c} \approx 2.0$. Equation (8) (with the radii converted to lattice units) yields the additional step edge barrier Δs , which amounts to 150_{-20}^{+40} meV, in good agreement with the result found above. For Pt(111), we use the data as given in Ref. 7. Growth at 425 K [see Fig. 2(b) in Ref. 7] yields islands with average separations of ~ 54 nm and widths of ~ 22 nm. We obtain from Eq. (8) an additional barrier of 165_{-20}^{+50} meV, in fair agreement with values obtained by effective-medium calculations.^{13,15}

We now consider the possible effects of Sb on the growth of Ag(111). Previously published explanations of the surfactant effect for this system^{6,16,20} have all relied on two assumptions; (i) that the mobility of Ag is limited by Sb and (ii) that Sb is not transported to the $(n+1)$ th layer until coalescence of the n th layer. This would indeed constitute a simple explanation: A higher mobility on top of islands would increase the interlayer transport through an increase in the attempt frequency and lead to smoother morphologies.²⁰ However, STM results show explicitly that this second assumption is false and that instead the Sb is transported continuously and with $\sim 95\%$ efficiency during growth, leading to a practically homogeneous distribution of Sb on all growing layers.^{8,12} This result clearly indicated that previous attempts at modeling this system have been oversimplified and inadequate.

The model developed above allows a more complete and quantitative understanding of the workings of Sb on this system. Specifically, we analyze the relative importance of three possible surfactant effects, (i) the increasing Ag diffusivity in higher layers due to partial incorporation of the Sb in the growing film,^{8,12} (ii) the formation of irregular island shapes,^{8,12} and (iii) the increased Ag diffusion barrier on the terraces.^{6,8,12,16}

(i) On the basis of the partial incorporation of Sb during growth, a decrease in island density with coverage is expected. Comparison of island densities observed in different layers, however, shows that the change from each layer to the next is small, indicating that this is not a strong effect. This can be quantified as follows. The observed exponential increase in the Ag island density with Sb coverage¹² implies a linear relation between Sb coverage and Ag diffusion barrier. Assuming a critical island size $i=1$ we estimate^{17,18} an increase in the Ag diffusion barrier of 15 meV per percent of a ML of Sb. Furthermore, our STM and Auger electron spectroscopy data show an Sb incorporation rate of 5% per ML of added Ag. Thus, for an Sb precoverage of 0.08 ML the decrease in the Ag diffusion barrier in moving from the first to the second layer is ~ 6 meV. This corresponds to a lowering of $R_{0,c}/R_{1,c}$ by less than 5% [Eq. (8)] and an onset of second-layer nucleation which is changed to a coverage less than 9% higher as compared to the clean case. This does not suffice to explain the change in growth mode.

(ii) Irregular Ag island shapes also favor interlayer transport, because the adatoms reach the island edges more easily than for compact island shapes. For an annealed Sb precoverage of 0.08 ML and an Ag coverage of 0.6 ML, STM images show irregular first-layer Ag islands without second-layer nucleation, with spacings of 150 nm ($R_{0,c} = 75$ nm) and centers of 80 nm diameter ($R_{1,c} \sim 40$ nm).¹² Using h_1/h_0 from above to include the effect discussed in (i), and leaving the additional barrier unchanged, Eq. (8) would predict second-layer nucleation already on islands with a radius of 20 nm. [The effect of irregular island shapes alone can be considered by using $h_1/h_0 = 1$ in Eq. (8).] Hence, these two effects in combination are too small to solely explain the transition to smooth growth.

(iii) It is the reduced mobility h , as implied by an increase in island density, which predominantly accounts for the observations of smoother growth. The Sb increases the effective diffusion barrier on terraces without affecting the total barrier for moving over step edges equally strongly. At an Sb coverage of 0.08 ML, the diffusion barrier has increased by ~ 120 meV.¹² With an unchanged edge barrier s , the ratio $R_{0,c}/R_{1,c}$ approaches unity and no second-layer nucleation is expected until a coverage of 0.99 ML is reached, even with relaxed island shapes. We conclude that the Sb-induced change in growth mode of Ag(111) can be fully explained on the basis of a decrease in additional barrier through an increase in diffusion barrier.¹⁹ Irregular island shapes or the partial incorporation of Sb from layer to layer^{6,16,20} are not sufficient to account for the observed change in growth.

Finally, for the reentrant layer growth of Pt on Pt(111) at low temperatures,^{2,7} we reach conclusions analogous to those for Sb/Ag(111). First of all, with lower temperature epitaxial growth usually becomes rougher. In the present model this is reflected in that the derivative of the ratio $R_{0,c}/R_{1,c}$

with respect to temperature is always negative. Hence, a transition to smoother growth upon lowering the temperature can occur only if either (i) the islands develop an irregular shape or (ii) the effectiveness of the additional barrier is decreased, for example, through small island sizes or kinks.² To consider the role of irregular island shapes, we apply Eq. (8) to the STM images taken at 205 K (Fig. 2a of Ref. 7). Assuming an additional barrier of 165 meV, as derived above, we find that second-layer islands would nucleate even if the island arms are only a single atom wide. Thus, the reported increase in interlayer transport at lower temperature cannot be due to purely geometric effects. Again, we must invoke a decrease in the effectiveness of the barrier at the step edge (ii), in this case either through kinks, transient energy,^{2,3,21} or downward funneling,²² to explain the smooth growth.

In conclusion, we have given an analytic description of epitaxial growth which brings to light the importance of the additional step edge energy barrier. The most important

qualitative result is that a decrease in the additional barrier, through an increase in the diffusion barrier on terraces, will increase interlayer transport and promote smoother growth morphologies. This will have important general implications for the choice of surfactant materials. Quantitatively, we have provided a demonstration of how this important barrier can be extracted from STM or LEEM images; for Ag(111) and Pt(111) these amount to roughly 150 and 165 meV, respectively. Finally, we have used the model to demonstrate that both for the cases of Sb surfactants on Ag(111) and for the reentrant smooth growth of Pt(111) at low temperature, reduced additional step edge barriers are the main cause of the smooth morphology.

We gratefully acknowledge financial support from the Alexander-von-Humboldt Foundation (J.A.M. and J.V.). Part of this work was supported by the Nederlandse Organisatie voor Wetenschappelijk Onderzoek (NWO) through the Stichting voor Fundamenteel Onderzoek der Materie (FOM).

¹M. T. Keif and W. F. Egelhoff, Jr., *Phys. Rev. B* **47**, 10 785 (1993), and references therein.

²B. Poelsema, R. Kunkel, N. Nagel, A. F. Becker, G. Rosenfeld, L. K. Verheij, and G. Comsa, *Appl. Phys. A* **53**, 369 (1991).

³W. F. Egelhoff, Jr. and D. A. Steigerwald, *J. Vac. Sci. Technol. A* **7**, 2167 (1989).

⁴H. A. van der Vegt, H. M. van Pinxteren, M. Lohmeier, E. Vlieg, and J. M. C. Thornton, *Phys. Rev. Lett.* **68**, 3335 (1992).

⁵S. Esch, M. Hohage, T. Michely, and G. Comsa, *Phys. Rev. Lett.* **72**, 518 (1994).

⁶J. Tersoff, A. W. Denier van der Gon, and R. M. Tromp, *Phys. Rev. Lett.* **72**, 266 (1994).

⁷M. Bott, T. Michely, and G. Comsa, *Surf. Sci.* **272**, 161 (1992).

⁸J. Vrijmoeth, J. A. Meyer, H. A. van der Vegt, E. Vlieg, and R. J. Behm, *Phys. Rev. Lett.* **72**, 3843 (1994).

⁹P. L. Cohen, G. S. Petrich, P. R. Pukite, G. J. Whaley, and A. S. Arrott, *Surf. Sci.* **216**, 222 (1989).

¹⁰S. Stoyanov and I. Markov, *Surf. Sci.* **116**, 313 (1982).

¹¹Z. Zhang and M. G. Lagally, *Phys. Rev. Lett.* **72**, 693 (1994).

¹²H. A. van der Vegt, J. Vrijmoeth, J. A. Meyer, R. J. Behm, and E. Vlieg (unpublished).

¹³Y. Li and A. E. DePristo, *Surf. Sci.* **319**, 141 (1994).

¹⁴J. A. Meyer and R. J. Behm, *Phys. Rev. Lett.* **73**, 364 (1994).

¹⁵J. Nørskov, *J. Condens. Matter.* **6**, 9495 (1994).

¹⁶S. Oppo, V. Fiorentini, and M. Scheffler, *Phys. Rev. Lett.* **71**, 2437 (1993).

¹⁷J. A. Venables, G. D. Spiller, and M. Hanbrücken, *Rep. Prog. Phys.* **47**, 399 (1984).

¹⁸M. C. Bartlett and J. W. Evans, *Phys. Rev. B* **46**, 12 675 (1992).

¹⁹It should be noted that our use of "increased diffusion barrier on terraces" could be more generally interpreted as a lower diffusivity on terraces due to any of several possible effects of the additive.

²⁰G. Rosenfeld, R. Servaty, C. Teichert, B. Poelsema, and G. Comsa, *Phys. Rev. Lett.* **71**, 895 (1993).

²¹P. Smilauer, M. R. Wilby, and D. D. Vvedensky, *Phys. Rev. B* **47**, 4119 (1993).

²²J. W. Evans, D. E. Sanders, P. A. Thiel, and A. E. DePristo, *Phys. Rev. B* **41**, 5410 (1990).